

Floquet Insulators and Lattice Fermions

Thomas Iadecola^{1,2,*} Srimoyee Sen^{1,†} and Lars Sivertsen^{1,‡}

¹*Department of Physics and Astronomy, Iowa State University, Ames, Iowa 50011, USA*

²*Ames National Laboratory, Ames, Iowa 50011, USA*



(Received 26 July 2023; accepted 7 March 2024; published 26 March 2024)

Floquet insulators are periodically driven quantum systems that can host novel topological phases as a function of the drive parameters. These new phases exhibit features reminiscent of fermion doubling in discrete-time lattice fermion theories. We make this suggestion concrete by mapping the spectrum of a noninteracting $(1+1)$ D Floquet insulator for certain drive parameters onto that of a discrete-time lattice fermion theory with a time-independent Hamiltonian. The resulting Hamiltonian is distinct from the Floquet Hamiltonian that generates stroboscopic dynamics. It can take the form of a discrete-time Su-Schrieffer-Heeger model with half the number of spatial sites of the original model, or of a $(1+1)$ D Wilson-Dirac theory with one quarter of the spatial sites.

DOI: 10.1103/PhysRevLett.132.136601

Zero-energy fermionic modes, or zero modes, are among the earliest manifestations of topology in quantum many-body theory. In systems with a gapped bulk, they appear localized at topological defects like solitons and vortices, or as dispersive modes at boundaries between phases with different bulk topological invariants [1]. They can carry fractional charges under global symmetries and manifest fractional or non-Abelian statistics when braided [2–7], and their existence enforces degeneracies in the many-body spectrum [8,9].

Quantum systems driven periodically in time, known as Floquet systems, furnish intrinsically nonequilibrium generalizations of topological and conventionally ordered phases [10–21]. Despite lacking energy conservation, they retain a notion of eigenstates and eigenvalues when observed at “stroboscopic times” that are integer multiples of the driving period T . Instead of an energy spectrum which can, in principle, be unbounded in the thermodynamic limit, stroboscopic dynamics and eigenstates are characterized by a bounded spectrum of quasienergies $-\pi/T \leq \epsilon < \pi/T$ that are only conserved modulo $(2\pi/T)$. The periodic nature of quasienergy furnishes a generalization of zero modes. For example, fermionic Floquet systems known as Floquet insulators can exhibit localized “ π modes” whose existence implies a “ π pairing” between many body states at quasienergy ϵ and $\epsilon + (\pi/T)$ [22–27].

Another setting in which π modes arise is spacetime lattice regularizations of fermionic quantum field theories. In particular, discretizing the Dirac operator on a spacetime lattice leads to the so-called fermion doubling problem, where the total number of fermionic degrees of freedom increases by a factor of 2^D , where D is the spacetime dimension [28,29]. The extra modes, known as “doubblers,” are undesirable and several methods, including Wilson,

Kogut-Susskind, and domain-wall fermions [30–35], are commonly used to dispense with them. Nevertheless, it is natural to ask whether the doubler modes associated with zero modes, which occur at frequency (π/τ) , where τ is the temporal lattice spacing, are related to the π modes that can appear in Floquet insulators.

In this Letter, we answer this question affirmatively for a particular $(1+1)$ D Floquet-insulator model. Specifically, we show that the quasienergy spectrum of a continuous-time Floquet model of spinless complex fermions can be

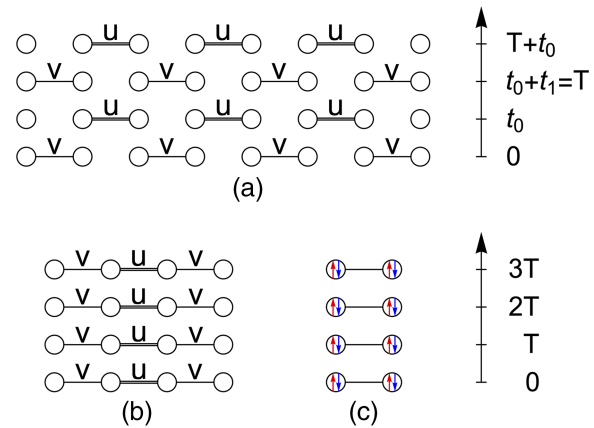


FIG. 1. Schematic of the mapping between stroboscopic Floquet dynamics and time-independent lattice Hamiltonians. The spectrum of the stroboscopic dynamics corresponding to Eq. (6), shown in (a), can be mapped onto that of a discrete-time Su-Schrieffer-Heeger (b) or Wilson-Dirac (c) theory. The number of spatial sites in (b) is halved with respect to (a) to accommodate the additional degrees of freedom due to fermion doubling. The number of sites are further halved in (c) to accommodate the spinful nature of the Wilson-Dirac fermions (depicted via arrows inside the lattice sites).

mapped directly onto the spectrum of discrete-time lattice fermions with a time-independent Hamiltonian. The lattice spacing of this discrete time theory equals the driving time period T of the Floquet system. The mapping is made easier by the observation that the Dirac equation takes the form of a Schrödinger equation for the corresponding fermion Hamiltonian. The lattice fermion model can take the form of a Su-Schrieffer-Heeger (SSH) model with half the spatial lattice sites of the Floquet model, or of a Wilson-Dirac model with one quarter of the sites (see Fig. 1 for a schematic of the mapping). Furthermore, for appropriately chosen solutions of the mapping between spectra, the phase diagrams of the Floquet and lattice models match. In particular, the topological phase of the Floquet model, which exhibits localized zero and π modes with open boundary conditions, coincides with the topological phase of the related lattice Hamiltonians, where π modes appear as doublers of zero modes. While previous studies [36,37] have used Floquet systems to provide new perspectives on lattice fermion doubling, here we focus on exposing a direct correspondence between the two.

Lattice fermion doubling.—A continuous-time free-fermion theory in Minkowski space with Hamiltonian H has the fermion or Dirac operator $\gamma_0(i\partial_t - H)$ from which we can extract the Schrödinger operator $i\partial_t - H$. The eigenvalues of this operator are $\pm\sqrt{p_0^2 - E^2}$, where p_0 is the Fourier variable conjugate to time t and E are the eigenvalues of H [38]. The zeroes of these eigenvalues at $p_0 = E$ correspond to poles of the fermion propagator $(i\partial_t - H)^{-1}\gamma_0^{-1}$. Discretizing time in this theory leads to fermion doubling [28,29]. To see this, let τ be the lattice spacing in the time direction. The poles of the discrete-time theory now satisfy $(1/\tau)\sin(p_0\tau) = E$, which leads to two solutions:

$$p_0 = \frac{1}{\tau}\sin^{-1}(E\tau) \quad \text{and} \quad p_0 = \frac{\pi}{\tau} - \frac{1}{\tau}\sin^{-1}(E\tau). \quad (1)$$

Thus, for every pole of the continuous-time propagator there are two poles of the discrete-time propagator [39–42]. In particular, for a zero mode of the continuous-time theory, the discrete-time theory has modes at $p_0 = 0$ and $p_0 = (\pi/\tau)$; the new π mode arises purely due to time discretization.

A corresponding phenomenon is also observed in Euclidean-time lattice field theory [43,44]. There, the Schrödinger operator in continuous time has eigenvalues $\pm\sqrt{p_0^2 + E^2}$, which, unlike the Minkowski theory, vanishes only at $p_0 = E = 0$. In this case, upon discretizing time, fermion doubling manifests itself as a degeneracy of Schrödinger eigenvalues. For instance, any eigenstate $|p_0, E\rangle$ with eigenvalue $(1/\tau)\sqrt{\sin^2(p_0\tau) + E^2}$ has a partner $|(\pi/\tau) - p_0, E\rangle$ with the same eigenvalue. In congruence with the Minkowski-space analysis, if the continuous-time fermion propagator has a pole at $p_0 = E = 0$, then

there is another pole at $p_0 = \pi/\tau$. More interestingly, the states $|(1/\tau)\sin^{-1}(E\tau), E\rangle$, which correspond to the energy eigenstates of H , have the same spatial profiles in the position eigenbasis as $|(\pi/\tau) - (1/\tau)\sin^{-1}(E\tau), E\rangle$. Therefore, if H has a spatially localized zero mode, the corresponding discrete-time Schrödinger equation has two solutions with the same spatial profile.

In this Letter, we will consider real-time (i.e., Minkowski) theories as opposed to imaginary-time (Euclidean) ones, as the comparison between the Floquet and lattice spectra is more natural for the former. However, there is no fundamental obstruction to performing a similar analysis for Euclidean theories, and such an approach may be desirable when generalizing beyond the case of noninteracting fermions, which is our focus here. We will briefly mention how the comparison between Floquet systems and lattice fermions in Minkowski spacetime can be adapted for Euclidean spacetime lattices.

Floquet insulator model.—As a simple example of a Floquet insulator, we consider a continuous-time $(1+1)$ D model on a spatial lattice of $2N$ sites defined by the evolution operator

$$U(t) = \begin{cases} e^{-iH_0 t} & \text{for } 0 < t < t_0 \\ e^{-iH_1(t-t_0)} e^{-iH_0 t_0} & \text{for } t_0 \leq t < t_0 + t_1 \end{cases}, \quad (2)$$

with

$$\begin{aligned} H_0 &= 2 \sum_{j=0}^{N-1} (a_{2j}^\dagger a_{2j+1} + \text{H.c.}) \\ H_1 &= 2 \sum_{j=0}^{N-1} (a_{2j+1}^\dagger a_{2j+2} + \text{H.c.}), \end{aligned} \quad (3)$$

where a_i is a fermion annihilation operator on site $i = 0, \dots, 2N - 1$. Unless otherwise specified, we consider periodic boundary conditions (PBC) such that $a_{2N} \equiv a_0$. The Hamiltonians in Eq. (3) are the “trivial” and “topological” parts of the (static) SSH model [2,51],

$$H_{\text{SSH}} = \frac{u}{2}H_1 + \frac{v}{2}H_0. \quad (4)$$

The energy spectrum of this model with PBC is given by

$$E_{\text{SSH}}(k) = \pm\sqrt{u^2 + v^2 + 2uv\cos(2k)}, \quad (5)$$

where $0 \leq k < \pi$ is the crystal momentum and we have set the spatial lattice spacing to 1. The SSH model has a symmetry-protected topological (SPT) and a trivial phase that have identical bulk spectra. The two gapped phases can be distinguished by their energy spectra in open boundary conditions (OBC): in the SPT phase there are two spatially localized zero modes pinned to the middle of the energy gap, one at each end of the chain, while in the trivial phase

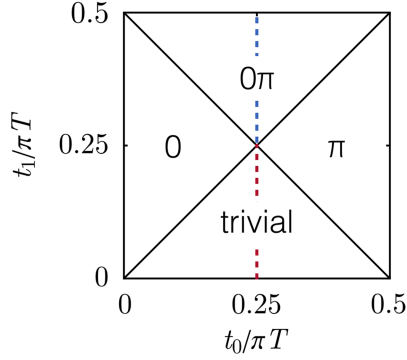


FIG. 2. Phase diagram of the Floquet model (6). The phases are labeled by the presence or absence of zero and π modes localized to boundaries. This Letter focuses on the vertical dashed line at $(t_0/T) = (\pi/4)$, which passes through the trivial and 0π phases.

there are none. Expanding the model around $k = (\pi/2)$ yields a Dirac fermion theory with a mass proportional to $u - v$; the transition between the SPT and trivial phases occurs at the massless point $u = v$. H_0 and H_1 can be viewed as representatives of the trivial and SPT phases, respectively.

The Floquet model (2) is closely related to a simple $(1+1)$ D model discussed in Refs. [24,27,52], with the small difference that Eq. (2) is formulated in terms of complex rather than Majorana fermion operators [53]. The analysis of both models is nearly identical, and they have the same phase diagram. Since energy is no longer conserved in the time-dependent model (2), phases are classified according to spectral properties of the Floquet operator

$$U_F = U(T) = e^{-iH_1 t_1} e^{-iH_0 t_0} \equiv e^{-iH_F T}, \quad (6)$$

where $T = t_0 + t_1$ is the driving period and $H_F = (i/T) \ln U_F$ is known as the Floquet or stroboscopic Hamiltonian. The quasienergies $-\pi/T \leq \epsilon < \pi/T$ are the eigenvalues of H_F . They can be obtained analytically because the model (6) is quadratic [53]. There are four phases, which we label trivial, 0, π , and 0π (see Fig. 2). The 0 and π phases have localized boundary modes with $\epsilon = 0$ and (π/T) , respectively; the 0π phase has both zero and π modes, while the trivial phase has neither. The phase boundaries in Fig. 2 are the lines in the t_0 - t_1 plane where the quasienergy gap closes. The trivial and 0 phases are adiabatically connected to the trivial and topological phases of the SSH model, respectively. The phases with π modes are “intrinsically Floquet” phases in the sense that they cannot arise in the absence of the drive.

Floquet to lattice mapping.—It is natural to speculate that the π modes in the Floquet system can be viewed as doubler modes of an appropriate discrete-time lattice fermion theory with time lattice constant $\tau = T$. To confirm this, we will identify a discrete-time theory with Hamiltonian H and spectrum E such that the poles in

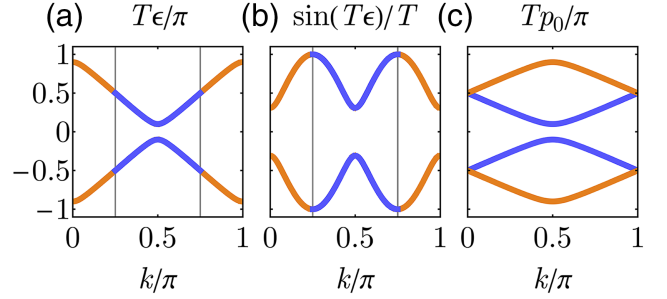


FIG. 3. Spectrum of the Floquet model and its mapping onto the lattice spectrum for $\eta = \pi/20$. (a) Quasienergy spectrum of Eq. (6) along the line $(t_0/T) = (\pi/4)$ [see Eq. (7)]. The quasienergy values highlighted in blue are those corresponding to crystal momenta k in the interval $[(\pi/4), (3\pi/4))$ (gray vertical lines), denoted $\tilde{\epsilon}$ in the text. (b) Sine-transformed quasienergy spectrum entering Eq. (8). (c) Pole positions p_0 with momenta assigned according to the SSH mapping. The orange bands denote doublers, which correspond to the quasienergies $(\pi/T) - \tilde{\epsilon}$.

Eq. (1) are in one-to-one correspondence with quasienergy eigenvalues ϵ . Note that, in order for this identification to be possible, it is necessary that the (single-particle) spectrum of H_F exhibit a π pairing such that for every quasienergy ϵ there is a partner at $(\pi/T) - \epsilon$. For the model (6), this feature arises along the line $(t_0/T) = (\pi/4)$, which connects the trivial and 0π phases. On this line, the quasienergy spectrum of H_F with PBC takes the form [53]

$$\epsilon(k) = \pm \cos^{-1}[-\cos(2\eta) \cos(2k)], \quad (7)$$

where $\eta = (t_1/T) - (\pi/4)$ measures the distance from the gap closure at $(t_1/T) = (\pi/4)$. To enable a one-to-one mapping onto the poles (1), we will partition the quasienergy spectrum ϵ into two subsets containing quasienergies $\tilde{\epsilon}$ and $(\pi/T) - \tilde{\epsilon}$. We will then seek a model H whose energy spectrum E satisfies

$$E = \frac{1}{T} \sin(T\tilde{\epsilon}), \quad (8)$$

which stems from identifying $p_0 = \tilde{\epsilon}$ in Eq. (1). A suitable choice of $\tilde{\epsilon}$ consists of the values $\epsilon(k)$ for $(\pi/4) \leq k < (3\pi/4)$ (see Fig. 3). The corresponding construction in Euclidean spacetime aims to identify the eigenvalues of the states $|(1/T)\sin^{-1}(ET), E\rangle$ and $|(\pi/T) - (1/T)\sin^{-1}(ET), E\rangle$ with $(1/T)\sqrt{2} \sin(T\tilde{\epsilon})$.

SSH mapping.—We now seek a Hamiltonian whose spectrum satisfies Eq. (8). Since U_F is built using the SSH-type Hamiltonians (3), we first consider an SSH Hamiltonian with dispersion given by Eq. (5). In this case, Eq. (8) can be solved by

$$E_{\text{SSH}}(k') = \frac{1}{T} \sin \left[T\epsilon \left(\frac{k'}{2} + \frac{\pi}{4} \right) \right], \quad (9)$$

where $0 \leq k' < \pi$, where

$$u = \frac{1 \pm \sin(2\eta)}{2T} \quad \text{and} \quad v = \frac{1}{T} - u. \quad (10)$$

(Note that we have assumed $u, v \geq 0$ for simplicity.)

The two possible assignments of u satisfying Eq. (9) have no impact on the bulk energy spectrum, but can nevertheless be physically distinguished by solving the SSH model with OBC. The SSH model (4) is in the SPT phase when $u > v$ and the trivial phase when $u < v$. Since the topological 0π phase of H_F occurs when $\eta > 0$, we must pick the branch of Eq. (10) such that $u > v$ when $\eta > 0$; this is accomplished by picking the “+” branch. Let \tilde{H}_{SSH} denote the resulting time-independent SSH Hamiltonian.

By construction, the doubled spectrum (1) of \tilde{H}_{SSH} when defined on a discrete-time lattice with spacing $\tau = T$ [Fig. 3(c)] matches the quasienergy spectrum of the Floquet Hamiltonian H_F [Fig. 3(a)]. Thus, \tilde{H}_{SSH} cannot be defined on the same spatial lattice as H_F ; rather, if the original Floquet model is defined on a lattice of $2N$ sites, \tilde{H}_{SSH} must be defined on N sites. To see this, recall that Eq. (9) maps the interval $(\pi/4) \leq k < (3\pi/4)$ to the interval $0 \leq k' < \pi$. The k interval contains half of the N allowed crystal momentum values for H_F , so k' can only take $(N/2)$ values (note that this requires N to be even). This corresponds to N sites because the SSH model has a two-site unit cell. Thus, \tilde{H}_{SSH} should not be interpreted as a mere rewriting of H_F . Instead, the models are related by the nontrivial procedure of fermion doubling.

Wilson-Dirac mapping.—To make more direct contact with lattice field theory, we now show that Eq. (8) can also be satisfied by the spectrum of a Wilson-Dirac (WD) Hamiltonian. The corresponding solution is inspired by the observation that the spectrum of a WD Hamiltonian with PBC can be mapped onto that of an SSH Hamiltonian with PBC. The WD Hamiltonian on a 1D spatial lattice with N sites can be written (here working in OBC for simplicity)

$$H_{\text{WD}} = \sum_{x,x'=0}^{N-1} \bar{\psi}_x \left[R\gamma_1(-i\nabla_{x,x'}) - \frac{R}{2}\nabla_{x,x'}^2 + m\delta_{x,x'} \right] \psi_{x'}, \quad (11)$$

where $\nabla_{x,x'} = (\delta_{x',x+1} - \delta_{x',x-1})/2$ is a symmetric spatial derivative, $\nabla_{x,x'}^2 = \delta_{x',x+1} + \delta_{x',x-1} - 2\delta_{x',x}$ is the second derivative, ψ_x is a two-component Dirac spinor with associated gamma matrices γ_0, γ_1 , and $\bar{\psi}_x = \psi_x^\dagger \gamma_0$. The energy spectrum of this model with PBC is given by

$$E_{\text{WD}}(p) = \pm \sqrt{R^2 \sin^2 p + [m + R(1 - \cos p)]^2}, \quad (12)$$

where $-\pi \leq p < \pi$. Solving Eq. (8) yields

$$E_{\text{WD}}(p') = \frac{1}{T} \sin \left[T\epsilon \left(\frac{p'}{4} + \frac{\pi}{2} \right) \right], \quad (13)$$

where $-\pi \leq p' < \pi$, provided that

$$m = \pm \frac{\sin(2\eta)}{T} \quad \text{and} \quad R = \frac{1}{2T} - \frac{m}{2}, \quad (14)$$

where we have assumed $R \geq 0$ for simplicity. Following the SSH case, we now ask which of these branches corresponds to a topological phase when $\eta > 0$. With OBC, the WD Hamiltonian (11) exhibits localized edge modes when $m < 0$ [53]. Demanding that this condition coincide with positive η selects the “−” branch. We denote the resulting time-independent Wilson-Dirac Hamiltonian by \tilde{H}_{WD} .

We have thus found a second time-independent Hamiltonian, \tilde{H}_{WD} , whose doubled spectrum when defined on a discrete-time lattice coincides with the quasienergy spectrum of H_F . We note here that \tilde{H}_{WD} must be defined on a lattice with $N/2$ sites (i.e., one-quarter of the sites in the original Floquet model). Like the SSH case, the crystal momentum interval $0 \leq k < (\pi/2)$ corresponding to $\tilde{\epsilon}$ contains $(N/2)$ points; thus, so does the new crystal momentum interval $-\pi \leq p' < \pi$. However, unlike the SSH model, the WD model has a one-site unit cell, so there is one site per crystal momentum value.

Discussion.—The equalities (9) and (13) relate the discrete-time spectra of static SSH and WD models to the quasienergy spectrum of Eq. (6) with PBC. In each case, the “correct” branch of the respective model parameter solutions is chosen by matching the presence of zero modes as a function of η . However, these zero modes are properties of the OBC spectrum. Given that the PBC spectra match by construction, we expect that the OBC spectra match up to $\sim 1/N$ corrections. In Fig. 4(a) we demonstrate this numerically for the SSH mapping by

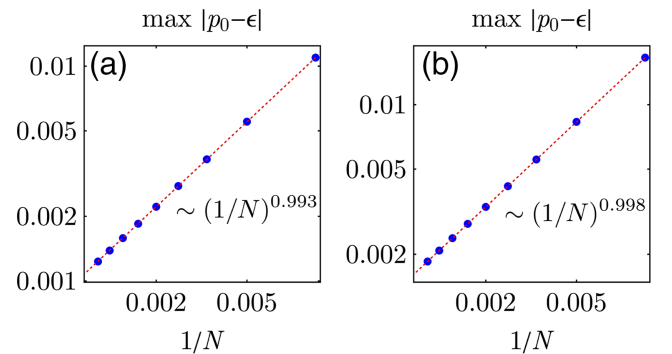


FIG. 4. Finite-size scaling of the maximum difference between discrete-time spectra p_0 and quasienergy spectra ϵ (a) for OBC and (b) for OBC with a domain wall where η switches sign. In both panels we compare to the SSH spectrum and fix $\eta = \pi/8$, considering system sizes $N = 100, 200, \dots, 900$. Dashed lines indicate best fits to power laws in $1/N$ that are consistent with the expected scaling.

plotting the system size dependence of the maximum difference between the discrete-time frequency spectrum p_0 and the quasienergy spectrum ϵ , where each spectrum is constructed as an ordered list.

Another test of equivalence is to compare spectra in the presence of a domain wall in η . For the SSH model, this corresponds to a standard domain wall in the mass profile [2], while for the WD model it amounts to a domain wall in both the mass and the Wilson parameter R . For the Floquet model, a domain wall in η entails an abrupt change in the coefficient of H_1 from 2 to $2[(\pi/4) - \eta]/[(\pi/4) + \eta]$ at some point in space. In Fig. 4(b) we examine the finite-size dependence of the difference between the discrete-time SSH and quasienergy spectra in the presence of a domain wall in the middle of the chain, again finding the expected $\sim 1/N$ scaling. Furthermore, we note that the spectral equivalence guarantees that the zero and π modes that appear at spatial boundaries and domain walls in all three models have matching localization lengths when the system size is scaled appropriately [53].

These results build confidence that the mapping we develop defines a notion of equivalence in the thermodynamic limit between models irrespective of boundary conditions or the presence of topological defects. Our mapping implies that any observable that depends on the single-particle Green's function, evaluated on the Floquet side at times $t = nT$, should match the corresponding observable in lattice field theory on the corresponding temporal lattice sites.

Outlook.—We have demonstrated spectral equivalence between a simple Floquet insulator model in $(1+1)$ dimensions and two canonical fermion models (SSH and WD) defined on a two-dimensional spacetime lattice. The π pairing in the single-particle spectrum, which occurs along the line $(t_0/T) = (\pi/4)$, allows us to discard half of the degrees of freedom in the Floquet model to define a related static model, which recovers the discarded eigenvalues via fermion doubling after time discretization. One interesting question for future work is whether the equivalence can be extended off the line $(t_0/T) = (\pi/4)$ [54]. We note that π pairing also occurs along the line $(t_1/T) = (\pi/4)$ for PBC but is lost for OBC, as evidenced by the separate existence of 0 and π modes with OBC. A separate direction is to consider extensions of these mappings to $(2+1)$ D systems, where new phases like anomalous Floquet topological insulators emerge [23,55]. In any dimension, it is also worth considering whether a similar equivalence between bulk topological invariants in Floquet systems [23,56–59] and lattice field theories can emerge [60]. Furthermore, it will be interesting to consider whether the conditions for destabilization of lattice topological phases in the presence of strong interactions and away from the continuum limit [61] can be related to the destabilization of Floquet phases due to unbounded heating.

The latter requires introducing prethermalization or localization physics to enable long-lived phenomena [24,62–64]. Finally, we note that our results may have implications for quantum simulation of lattice gauge theories. Indeed, gauge fields can be simulated in Floquet systems [65,66], and adding fermionic degrees of freedom with appropriate driving can potentially be used to mimic the fermionic sector of the discrete spacetime lattice field theory.

T. I. acknowledges support from the National Science Foundation under Grant No. DMR-2143635. S. S. and L. S. acknowledge support from the U.S. Department of Energy, Nuclear Physics Quantum Horizons program through the Early Career Award No. DE-SC0021892. We also thank Marina K. Marinkovic for alerting us to the possible application of our work to quantum simulations.

*iadecola@iastate.edu

†srimoyee08@gmail.com

‡lars@iastate.edu

- [1] J. C. Y. Teo and C. L. Kane, Topological defects and gapless modes in insulators and superconductors, *Phys. Rev. B* **82**, 115120 (2010).
- [2] R. Jackiw and C. Rebbi, Solitons with fermion number $\frac{1}{2}$, *Phys. Rev. D* **13**, 3398 (1976).
- [3] R. Jackiw and P. Rossi, Zero modes of the vortex-fermion system, *Nucl. Phys.* **B190**, 681 (1981).
- [4] C.-Y. Hou, C. Chamon, and C. Mudry, Electron fractionalization in two-dimensional graphenelike structures, *Phys. Rev. Lett.* **98**, 186809 (2007).
- [5] G. Moore and N. Read, Non-Abelions in the fractional quantum Hall effect, *Nucl. Phys.* **B360**, 362 (1991).
- [6] N. Read and D. Green, Paired states of fermions in two dimensions with breaking of parity and time-reversal symmetries and the fractional quantum Hall effect, *Phys. Rev. B* **61**, 10267 (2000).
- [7] D. A. Ivanov, Non-Abelian statistics of half-quantum vortices in p -wave superconductors, *Phys. Rev. Lett.* **86**, 268 (2001).
- [8] P. Fendley, Parafermionic edge zero modes in z_n -invariant spin chains, *J. Stat. Mech.* (2012) P11020.
- [9] P. Fendley, Strong zero modes and eigenstate phase transitions in the XYZ/interacting majorana chain, *J. Phys. A* **49**, 30LT01 (2016).
- [10] J. Cayssol, B. Dóra, F. Simon, and R. Moessner, Floquet topological insulators, *Phys. Status Solidi RRL* **7**, 101 (2013).
- [11] M. S. Rudner and N. H. Lindner, Band structure engineering and non-equilibrium dynamics in Floquet topological insulators, *Nat. Rev. Phys.* **2**, 229 (2020).
- [12] K. Sacha and J. Zakrzewski, Time crystals: A review, *Rep. Prog. Phys.* **81**, 016401 (2017).
- [13] D. V. Else, C. Monroe, C. Nayak, and N. Y. Yao, Discrete time crystals, *Annu. Rev. Condens. Matter Phys.* **11**, 467 (2020).
- [14] V. Khemani, R. Moessner, and S. L. Sondhi, A brief history of time crystals (2019).

- [15] J. Zhang, P. W. Hess, A. Kyprianidis, P. Becker, A. Lee, J. Smith, G. Pagano, I.-D. Potirniche, A. C. Potter, A. Vishwanath, N. Y. Yao, and C. Monroe, Observation of a discrete time crystal, *Nature (London)* **543**, 217 (2017).
- [16] S. Choi, J. Choi, R. Landig, G. Kucsko, H. Zhou, J. Isoya, F. Jelezko, S. Onoda, H. Sumiya, V. Khemani, C. von Keyserlingk, N. Y. Yao, E. Demler, and M. D. Lukin, Observation of discrete time-crystalline order in a disordered dipolar many-body system, *Nature (London)* **543**, 221 (2017).
- [17] A. Kyprianidis, F. Machado, W. Morong, P. Becker, K. S. Collins, D. V. Else, L. Feng, P. W. Hess, C. Nayak, G. Pagano, N. Y. Yao, and C. Monroe, Observation of a prethermal discrete time crystal, *Science* **372**, 1192 (2021).
- [18] X. Mi *et al.*, Time-crystalline eigenstate order on a quantum processor, *Nature (London)* **601**, 531 (2021).
- [19] P. T. Dumitrescu, J. G. Bohnet, J. P. Gaebler, A. Hankin, D. Hayes, A. Kumar, B. Neyenhuis, R. Vasseur, and A. C. Potter, Dynamical topological phase realized in a trapped-ion quantum simulator, *Nature (London)* **607**, 463 (2022).
- [20] X. Zhang *et al.*, Digital quantum simulation of Floquet symmetry-protected topological phases, *Nature (London)* **607**, 468 (2022).
- [21] J. W. McIver, B. Schulte, F.-U. Stein, T. Matsuyama, G. Jotzu, G. Meier, and A. Cavalleri, Light-induced anomalous Hall effect in graphene, *Nat. Phys.* **16**, 38 (2019).
- [22] M. Thakurathi, A. A. Patel, D. Sen, and A. Dutta, Floquet generation of majorana end modes and topological invariants, *Phys. Rev. B* **88**, 155133 (2013).
- [23] M. S. Rudner, N. H. Lindner, E. Berg, and M. Levin, Anomalous edge states and the bulk-edge correspondence for periodically driven two-dimensional systems, *Phys. Rev. X* **3**, 031005 (2013).
- [24] V. Khemani, A. Lazarides, R. Moessner, and S. L. Sondhi, Phase structure of driven quantum systems, *Phys. Rev. Lett.* **116**, 250401 (2016).
- [25] D. V. Else, B. Bauer, and C. Nayak, Floquet time crystals, *Phys. Rev. Lett.* **117**, 090402 (2016).
- [26] D. V. Else and C. Nayak, Classification of topological phases in periodically driven interacting systems, *Phys. Rev. B* **93**, 201103(R) (2016).
- [27] C. W. von Keyserlingk and S. L. Sondhi, Phase structure of one-dimensional interacting Floquet systems. I. Abelian symmetry-protected topological phases, *Phys. Rev. B* **93**, 245145 (2016).
- [28] H. B. Nielsen and M. Ninomiya, Absence of neutrinos on a lattice. 1. Proof by homotopy theory, *Nucl. Phys.* **B185**, 20 (1981); **B195**, 541(E) (1982).
- [29] H. B. Nielsen and M. Ninomiya, Absence of neutrinos on a lattice. 2. Intuitive topological proof, *Nucl. Phys.* **B193**, 173 (1981).
- [30] D. B. Kaplan, A Method for simulating chiral fermions on the lattice, *Phys. Lett. B* **288**, 342 (1992).
- [31] Y. Shamir, Chiral fermions from lattice boundaries, *Nucl. Phys.* **B406**, 90 (1993).
- [32] P. H. Ginsparg and K. G. Wilson, A remnant of chiral symmetry on the lattice, *Phys. Rev. D* **25**, 2649 (1982).
- [33] H. Neuberger, Exactly massless quarks on the lattice, *Phys. Lett. B* **417**, 141 (1998).
- [34] H. Neuberger, More about exactly massless quarks on the lattice, *Phys. Lett. B* **427**, 353 (1998).
- [35] J. Kogut and L. Susskind, Hamiltonian formulation of wilson's lattice gauge theories, *Phys. Rev. D* **11**, 395 (1975).
- [36] X.-Q. Sun, M. Xiao, T. Bzdušek, S.-C. Zhang, and S. Fan, Three-dimensional chiral lattice fermion in Floquet systems, *Phys. Rev. Lett.* **121**, 196401 (2018).
- [37] M. DeMarco and X.-G. Wen, A single right-moving free fermion mode on an ultralocal 1 + 1d spacetime lattice (2018).
- [38] Unless indicated otherwise, we restrict our focus in this work to single-particle spectral properties rather than many-body ones.
- [39] D. Bödeker, G. D. Moore, and K. Rummukainen, Chern-Simons number diffusion and hard thermal loops on the lattice, *Phys. Rev. D* **61**, 056003 (2000).
- [40] J. Ambjorn, T. Askgaard, H. Porter, and M. E. Shaposhnikov, Sphaleron transitions and baryon asymmetry: A numerical real time analysis, *Nucl. Phys.* **B353**, 346 (1991).
- [41] G. Aarts and J. Smit, Real time dynamics with fermions on a lattice, *Nucl. Phys.* **B555**, 355 (1999).
- [42] Z.-G. Mou, P. M. Saffin, and A. Tranberg, Ensemble fermions for electroweak dynamics and the fermion pre-heating temperature, *J. High Energy Phys.* **11** (2013) 097.
- [43] L. H. Karsten, Lattice fermions in euclidean space-time, *Phys. Lett. B* **104**, 315 (1981).
- [44] Typical lattice Monte Carlo studies of quantum field theories are performed in Euclidean space-time. For real-time formulations path integrals for quantum field theories and quantum mechanical systems see Refs. [45–50].
- [45] G. Kanwar and M. L. Wagman, Real-time lattice gauge theory actions: Unitarity, convergence, and path integral contour deformations, *Phys. Rev. D* **104**, 014513 (2021).
- [46] A. Alexandru, G. Basar, P. F. Bedaque, S. Vartak, and N. C. Warrington, Monte Carlo study of real time dynamics on the lattice, *Phys. Rev. Lett.* **117**, 081602 (2016).
- [47] S. Lawrence and Y. Yamauchi, Normalizing flows and the real-time sign problem, *Phys. Rev. D* **103**, 114509 (2021).
- [48] Y. Tanizaki and T. Koike, Real-time Feynman path integral with Picard-Lefschetz theory and its applications to quantum tunneling, *Ann. Phys. (Amsterdam)* **351**, 250 (2014).
- [49] A. Alexandru, G. Basar, P. F. Bedaque, and G. W. Ridgway, Schwinger-Keldysh formalism on the lattice: A faster algorithm and its application to field theory, *Phys. Rev. D* **95**, 114501 (2017).
- [50] Z.-G. Mou, P. M. Saffin, A. Tranberg, and S. Woodward, Real-time quantum dynamics, path integrals and the method of thimbles, *J. High Energy Phys.* **06** (2019) 094.
- [51] W. P. Su, J. R. Schrieffer, and A. J. Heeger, Solitons in polyacetylene, *Phys. Rev. Lett.* **42**, 1698 (1979).
- [52] A. C. Potter, T. Morimoto, and A. Vishwanath, Classification of interacting topological Floquet phases in one dimension, *Phys. Rev. X* **6**, 041001 (2016).
- [53] See Supplemental Material at <http://link.aps.org/supplemental/10.1103/PhysRevLett.132.136601> for a derivation of the quasienergy spectrum of H_F , a description of the phase diagram for the Floquet operator U_F and a discussion of a Wilson-Dirac fermion in 1 + 1 dimensions with a domain wall in the parameter η .

- [54] T. Iadecola, S. Sen, and L. Sivertsen, Floquet insulators and lattice fermions beyond naive time discretization, *Phys. Rev. Res.* **6**, 013098 (2024).
- [55] H. C. Po, L. Fidkowski, A. Vishwanath, and A. C. Potter, Radical chiral Floquet phases in a periodically driven Kitaev model and beyond, *Phys. Rev. B* **96**, 245116 (2017).
- [56] T. Kitagawa, E. Berg, M. Rudner, and E. Demler, Topological characterization of periodically driven quantum systems, *Phys. Rev. B* **82**, 235114 (2010).
- [57] F. Nathan and M. S. Rudner, Topological singularities and the general classification of Floquet-Bloch systems, *New J. Phys.* **17**, 125014 (2015).
- [58] D. Carpentier, P. Delplace, M. Fruchart, and K. Gawędzki, Topological index for periodically driven time-reversal invariant 2D systems, *Phys. Rev. Lett.* **114**, 106806 (2015).
- [59] M. Fruchart, Complex classes of periodically driven topological lattice systems, *Phys. Rev. B* **93**, 115429 (2016).
- [60] M. F. L. Golterman, K. Jansen, and D. B. Kaplan, Chern-Simons currents and chiral fermions on the lattice, *Phys. Lett. B* **301**, 219 (1993).
- [61] D. B. Kaplan, Chiral symmetry and lattice fermions, in *Les Houches Summer School: Session 93: Modern perspectives in lattice QCD: Quantum field theory and high performance computing* (2009), pp. 223–272, [arXiv:0912.2560](#).
- [62] P. Ponte, A. Chandran, Z. Papić, and D. A. Abanin, Periodically driven ergodic and many-body localized quantum systems, *Ann. Phys. (Amsterdam)* **353**, 196 (2015).
- [63] L. D'Alessio and M. Rigol, Long-time behavior of isolated periodically driven interacting lattice systems, *Phys. Rev. X* **4**, 041048 (2014).
- [64] D. V. Else, B. Bauer, and C. Nayak, Prethermal phases of matter protected by time-translation symmetry, *Phys. Rev. X* **7**, 011026 (2017).
- [65] N. Goldman and J. Dalibard, Periodically driven quantum systems: Effective Hamiltonians and engineered gauge fields, *Phys. Rev. X* **4**, 031027 (2014).
- [66] C. Schweizer, F. Grusdt, M. Berngruber, L. Barbiero, E. Demler, N. Goldman, I. Bloch, and M. Aidelsburger, Floquet approach to $\{BbbZ\}$ 2 lattice gauge theories with ultracold atoms in optical lattices, *Nat. Phys.* **15**, 1168 (2019).